

Why Do Enolate Anions Favor O-Alkylation over C-Alkylation in the Gas Phase? The Roles of Resonance and Inductive Effects in the Gas-Phase S_N2 Reaction between the Acetaldehyde Enolate Anion and Methyl Fluoride

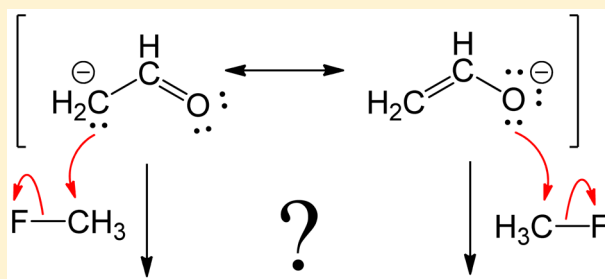
Christian G. Seitz,[†] Huaiyu Zhang,[‡] Yirong Mo,^{*,‡} and Joel M. Karty^{*,†}

[†]Department of Chemistry, Elon University, Elon, North Carolina 27244, United States

[‡]Department of Chemistry, Western Michigan University, Kalamazoo, Michigan 49008, United States

S Supporting Information

ABSTRACT: Contributions by resonance and inductive effects toward the net activation barrier were determined computationally for the gas-phase S_N2 reaction between the acetaldehyde enolate anion and methyl fluoride, for both O-methylation and C-methylation, in order to understand why this reaction favors O-methylation. With the use of the vinyllogue extrapolation methodology, resonance effects were determined to contribute toward increasing the size of the barrier by about 9.5 kcal/mol for O-methylation and by about 21.2 kcal/mol for C-methylation. Inductive effects were determined to contribute toward increasing the size of the barrier by about 1.7 kcal/mol for O-methylation and 4.2 kcal/mol for C-methylation. Employing our block-localized wave function methodology, we determined the contributions by resonance to be 12.8 kcal/mol for O-methylation and 22.3 kcal/mol for C-methylation. Thus, whereas inductive effects have significant contributions, resonance is the dominant factor that leads to O-methylation being favored. More specifically, resonance serves to increase the size the barrier for C-methylation significantly more than it does for O-methylation.



■ INTRODUCTION

Enolate anions are ambident nucleophiles in which the negative charge is delocalized over the oxygen atom and the α carbon atom. They can therefore undergo S_N2 alkylation at either atom, producing new C–C or O–C bonds, according to Scheme 1 for the acetaldehyde enolate anion.

The favored site of attack in these reactions depends on the particular reaction conditions. In solution, enolate anions tend to undergo C-alkylation, which makes them particularly valuable intermediates for the formation of new C–C bonds in organic synthesis.¹ Even though the enolate anion's dominant resonance contributor is the one with the negative charge on oxygen, strong solvation of the oxygen in a protic solvent reduces oxygen's nucleophilicity, leaving the α carbon as the preferred alkylation site.^{2,3} Yamataka and co-workers,⁴ furthermore, showed that the coordination of the metal counterion hinders O-methylation.

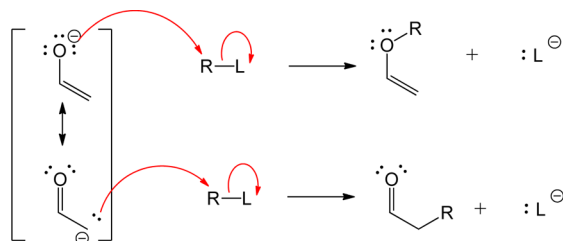
In the gas phase, on the other hand, enolate anions favor O-alkylation, as evidenced experimentally by Ellison and co-workers,³ who showed that the gas-phase S_N2 reaction between the cyclohexanone enolate anion and methyl bromide yields the O-methylated product exclusively. Computationally, Houk and Paddon-Row⁵ showed that, in the gas-phase reaction between acetaldehyde enolate and methyl fluoride, the energy barrier is lower for O-methylation than for C-methylation, even though the C-methylation product is thermodynamically favored. Because these studies were carried out in the gas phase, the

solvent and counterion effects described above are absent,⁶ revealing the intrinsic reactivity of the enolate.⁷

The lower energy barrier for O-alkylation than C-alkylation has been described from the perspective of Marcus theory.^{8–13} According to Marcus theory, the reaction energy barrier for an S_N2 reaction is governed by an intrinsic energy barrier (i.e., in which the transition state is located at the crossing of the reactant and product energy surfaces, assuming a thermoneutral reaction) as well as the energy difference between reactants and products. Namely, because C-alkylation leads to the thermodynamically favored product, the lower energy barrier of O-alkylation of acetaldehyde enolate in the gas phase must be due to a lower intrinsic energy barrier for that pathway. Indeed, Mayr and co-workers¹⁴ calculated the intrinsic energy barrier for the identity exchange S_N2 reactions for both O-methylation and C-methylation of acetaldehyde enolate and found that the intrinsic energy barrier for O-methylation is about 22 kcal/mol smaller than that for C-methylation. This mirrors the results by Rozenal and co-workers,¹⁵ who calculated the intrinsic energy barrier for the $\text{CH}_3\text{O}^- + \text{CH}_3-\text{OCH}_3$ identity exchange S_N2 reaction to be about 25 kcal/mol lower than the analogous $\text{H}_3\text{CCH}_2^- + \text{CH}_3-\text{CH}_2\text{CH}_3$ reaction. In the same vein, it is worth pointing out that Houk and Paddon-Row⁵ showed that the S_N2 reactions involving

Received: February 17, 2016

Published: March 24, 2016

Scheme 1. O-Alkylation versus C-Alkylation^a

^a(Left) The two resonance structures of the acetaldehyde enolate anion. (Top) O-alkylation is shown to take place with a generic substrate, producing an enol ether. (Bottom) C-alkylation is shown to take place with a generic substrate, producing an α -alkylated product.

CH_3F exhibit a lower energy barrier when HO^- is the nucleophile than when H_3C^- is the nucleophile.

Even though the regioselectivity of enolate alkylation can be presented in terms of Marcus theory, there are important effects that still need to be accounted for, in a direct fashion, to provide a complete understanding of *why* O-alkylation is favored over C-alkylation in the gas phase. Resonance, for example, should play an important role, as shown in Figure 1a. Resonance in the enolate nucleophile provides substantial stabilization that can be impacted differently along the reaction coordinates for C- versus O-alkylation. Moreover, as shown in Figure 1b, inductive effects should play a role, too. Each localized resonance structure of the enolate anion exhibits an inductively electron-withdrawing substituent directly attached to the nucleophilic atom, which will impact the concentration of negative charge on the nucleophilic atom. This is seen relatively easily in the second resonance structure in Figure 1b, which exhibits an electronegative oxygen atom near the nucleophilic carbon atom. But inductive effects are expected in the first resonance structure, too. The nucleophilic oxygen atom is attached to an sp^2 -hybridized carbon that has an enhanced effective electronegativity due to its s -character. In fact, we have previously shown that such an inductive effect can be substantial.¹⁶

Our present study therefore aims to quantify the contributions by resonance and inductive effects toward the energy barriers for the gas-phase C- and O-alkylation of an enolate. To our knowledge, we are the first to do so. We have chosen the reaction between acetaldehyde enolate and methyl fluoride as the model system and we applied two different computational methodologies to study it: vinylogue extrapolation and block-localized wave functions. Both of these methodologies are described below.

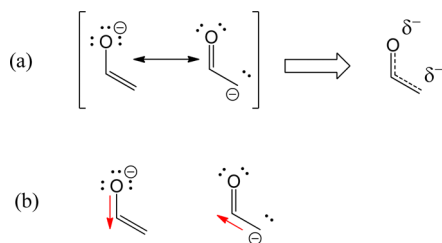


Figure 1. Resonance and inductive effects in the enolate anion. (a) Resonance delocalization in the enolate anion gives the O and C atoms partial negative charges. (b) In each resonance structure of the enolate anion, the negatively charged atom is directly attached to an inductively electron-withdrawing substituent.

THE DOUBLE-WELL POTENTIAL ENERGY SURFACE FOR GAS-PHASE $\text{S}_{\text{N}}2$ REACTIONS

Olmstead and Brauman¹⁷ showed that the double-well potential in Figure 2 describes gas-phase $\text{S}_{\text{N}}2$ reactions involving negatively charged nucleophiles. As the distance between the reactants decreases, attractive ion–dipole forces cause the energy to decrease to a local energy minimum, corresponding to the reactant ion–dipole complex, $\text{Nu}^- \bullet \text{R-L}$. The ion–dipole complex forms prior to any substantial bond breaking or forming. Energy then rises as the Nu-R bond begins to form and the R-L bond begins to break, until the transition state is reached at the local maximum. Continuing along the reaction coordinate, energy decreases to the local minimum corresponding to the product ion–dipole complex prior to separation of the product species.

Given the double-well potential, there are two ways the energy barrier for the reaction can be computed. One is the central activation barrier, E^* , which is the energy difference between the reactant ion–dipole complex and the transition state, and the other is the net activation barrier, E^b , which is the energy difference between the separated reactants and the transition state. In our previous study of the benzylic effect,¹⁸ values of E^b were used for comparison instead of E^* in order to avoid complications from intermolecular forces contributing unequally to the various ion–dipole complexes. Comparisons will be made among E^b values in the present study, too.

COMPUTATIONAL METHODOLOGIES

Vinylogue Extrapolation (VE). The vinylogue extrapolation (VE) methodology has been described elsewhere.^{16,19–21} As it applies to the present study, the energies of the transition state and the separated reactant species are calculated for each $\text{S}_{\text{N}}2$ reaction of acetaldehyde enolate with methyl fluoride, and E^b is obtained by subtracting the energy of the transition state from the sum of the energies of the separated reactant species. These calculations are repeated with *parallel vinylogues*, *perpendicular vinylogues*, and *reference vinylogues* of the parent nucleophile and transition state species, which are shown in Figures 3 and 4. Each parallel vinylogue is constructed by inserting n vinyl groups between the nucleophilic atom and the attached group responsible for resonance and inductive effects (i.e., the $\text{CH}=\text{CH}_2$ group in O-methylation and the $\text{CH}=\text{O}$ group in C-methylation), ensuring that the π system along the chain is entirely coplanar. Each perpendicular vinylogue is obtained by rotating the group responsible for resonance and inductive effects perpendicular to the remaining conjugated chain. Reference vinylogues are constructed by replacing the group responsible for resonance and inductive effects with a hydrogen atom.

Values of E^b are calculated for the $n = 1-5$ parallel, perpendicular, and reference vinylogues, denoted $E^b_{n,\text{par}}$, $E^b_{n,\text{perp}}$, and $E^b_{n,\text{ref}}$ respectively. Because orthogonal π systems effectively do not interact via resonance, the difference in E^b between analogous (i.e., same n) parallel and perpendicular vinylogues is the contribution by resonance toward E^b for that value of n , denoted $\Delta E^b_{\text{res}}(n)$, according to eq 1. Because hydrogen does not contribute via resonance or inductive effects, the difference in E^b between analogous perpendicular and reference vinylogues is the contribution by inductive effects toward E^b for that value of n , denoted $\Delta E^b_{\text{ind}}(n)$, according to eq 2.

$$\Delta E^b_{\text{res}}(n) = E^b_{n,\text{perp}} - E^b_{n,\text{par}} \quad (1)$$

$$\Delta E^b_{\text{ind}}(n) = E^b_{n,\text{ref}} - E^b_{n,\text{perp}} \quad (2)$$

Values of $\Delta E^b_{\text{res}}(n)$ and $\Delta E^b_{\text{ind}}(n)$ are determined for $n = 1-5$ and are separately extrapolated back to $n = 0$, which represents the parent enolate reaction systems.

Block-Localized Wave Function (BLW). The concept of resonance applies when a single Lewis structure cannot appropriately

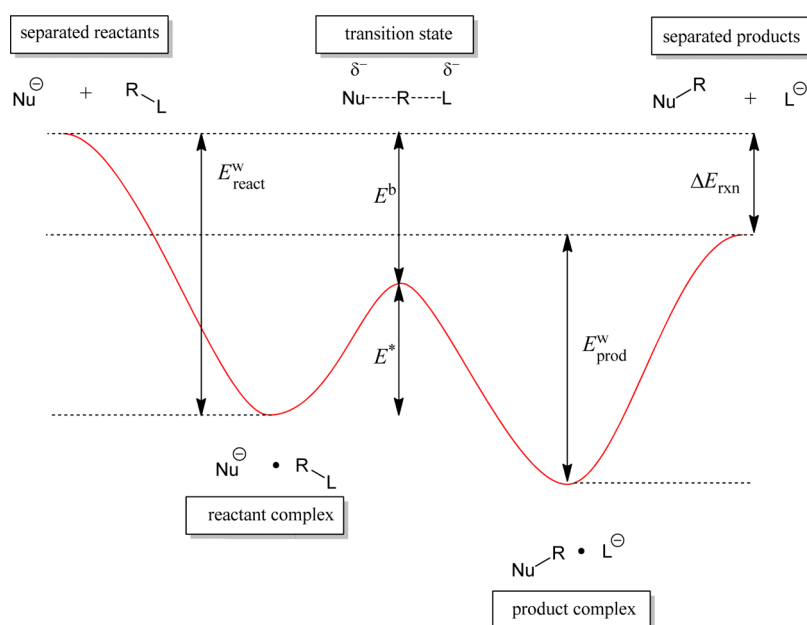


Figure 2. The double-well potential energy surface for a gas-phase S_N2 reaction. Complexation energies of the reactant and product complexes are denoted E^w_{react} and E^w_{prod} , respectively. The central activation barrier is denoted E^* , and the net activation barrier is denoted E^b .

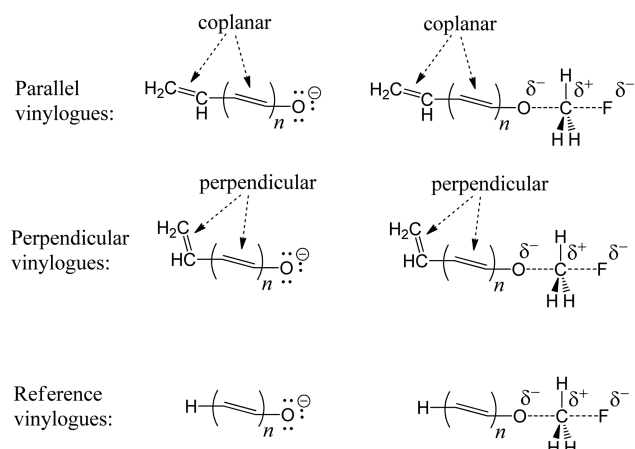


Figure 3. Vinylogues in O-methylation. Parallel and perpendicular vinylogues are constructed by inserting n vinyl groups between the nucleophilic oxygen and the attached $\text{CH}=\text{CH}_2$. In the parallel vinylogues, the entire conjugated chain is coplanar. In the perpendicular vinylogues, the terminal $\text{CH}=\text{CH}_2$ group is perpendicular to the rest of the conjugated chain. Reference vinylogues are constructed by replacing the terminal $\text{CH}=\text{CH}_2$ group with H.

describe the physicochemical properties and structural parameters of a molecule.^{22,23} In other words, a conjugated system is described with several electron-localized Lewis structures. Accordingly, in the ab initio valence bond (VB) theory, a molecular wave function is expressed as a superposition of several Heitler-London-Slater-Pauling (HLSP) functions, each of which corresponds to a Lewis structure.^{24–27} However, due to the fast increasing number of Slater determinants involved in each HLSP function and the nonorthogonality of orbitals, the computations of the Hamiltonian and overlap matrix elements between HLSP functions remain the challenging task for ab initio VB methods.²⁷ One way to significantly reduce the computational costs is through the use of nonorthogonal doubly occupied bond orbitals which were later generalized to fragment-localized orbitals.^{28–35} In the BLW method, where a BLW corresponds to an electron-localized diabatic state,^{36–38} it is assumed that the total electrons and primitive basis functions can be divided into several subgroups (blocks), and each MO

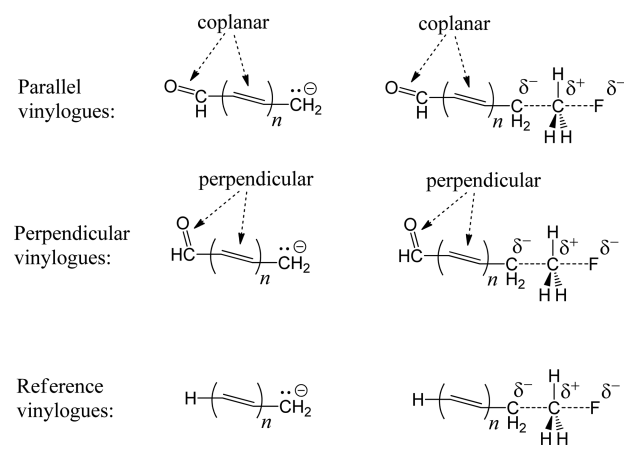


Figure 4. Vinylogues in C-methylation. Parallel and perpendicular vinylogues are constructed by inserting n vinyl groups between the nucleophilic carbon and the attached $\text{CH}=\text{O}$. In the parallel vinylogues, the entire conjugated chain is coplanar. In the perpendicular vinylogues, the terminal $\text{CH}=\text{O}$ group is perpendicular to the rest of the conjugated chain. Reference vinylogues are constructed by replacing the terminal $\text{CH}=\text{O}$ group with H.

φ_{ij} is block-localized and expanded in only one block i whose subspace is composed of m_i basis functions $\{\chi_{i\mu}\}$ as

$$\varphi_{ij} = \sum_{\mu=1}^{m_i} C_{ij\mu} \chi_{i\mu} \quad (3)$$

Subsequently, the BLW is defined using a Slater determinant, and in the closed-shell case

$$\Psi^{\text{BLW}} = M \det(\varphi_{11}^2 \varphi_{12}^2 \cdots \varphi_{1(n_1/2)}^2 \varphi_{21}^2 \cdots \varphi_{i1}^2 \cdots \varphi_{i(n_i/2)}^2 \cdots \varphi_{k(n_k/2)}^2)^{1/2} \\ = M \hat{A}[\Phi_1 \cdots \Phi_i \cdots \Phi_k] \quad (4)$$

where Φ_i is the direct product of block-localized orbitals in block i . Orbitals in the same subspace are subject to the orthogonality constraint, similar to MO theory, but orbitals belonging to different subspaces are nonorthogonal, a characteristic in VB theory. Since Kohn–Sham DFT has a self-consistent procedure identical to the HF method except that

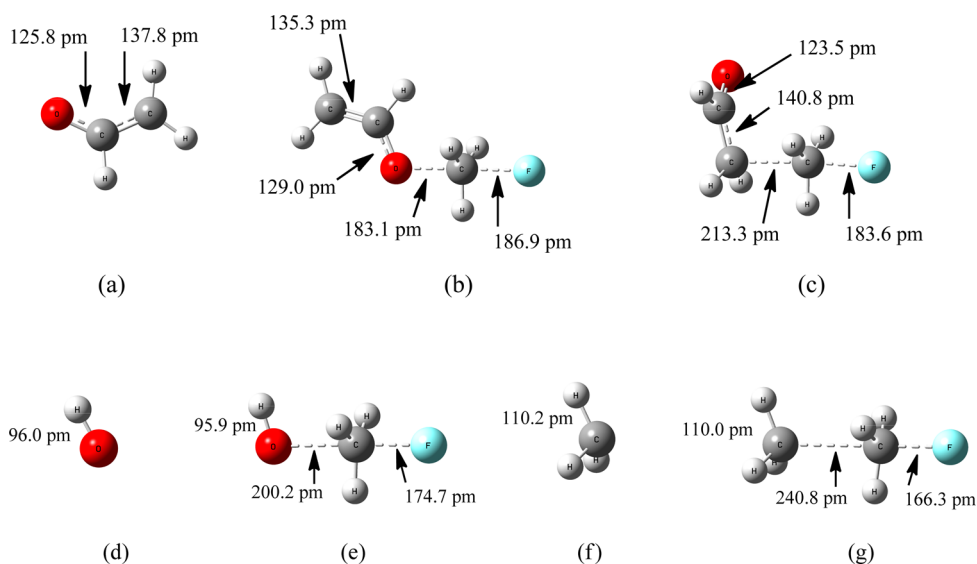


Figure 5. Optimized geometries at the MPW1PW91/6-311++G(3df,3pd) level of theory are shown for: (a) acetaldehyde enolate, (b) the transition state for O-methylation of acetaldehyde enolate with CH_3F , (c) the transition state for C-methylation of acetaldehyde enolate with CH_3F , (d) hydroxide anion, (e) the transition state for the reaction of hydroxide anion with CH_3F , (f) methanide anion, and (g) the transition state for the reaction of methanide anion with CH_3F .

the HF exchange potential is replaced by a DFT exchange-correlation (XC) potential, the BLW method can be straightforwardly extended to the DFT level.³⁷ Thus, for each resonance structure, we can construct a BLW. But we also understand that a delocalized wave function from MO or DFT methods is essentially a combination of all resonance structures. As such, the resonance energy can be defined as the energy difference between a MO or DFT state and the BLW state as

$$\Delta E_{\text{res}} = E(\Psi^{\text{DFT}}) - E(\Psi^{\text{BLW}}) \quad (5)$$

COMPUTATIONAL DETAILS

Vinylogue Extrapolation (VE). For the VE method, molecular orbital calculations were employed using the Gaussian 09 and GaussView5 software packages.^{39,40} These calculations were carried out with density functional theory at the MPW1PW91 level of theory (Barone's modified Perdew-Wang 1991 exchange functional and Perdew and Wang's 1991 correlation functional),⁴¹ using the 6-311++G(3df,3pd) basis set. This level of theory and basis set were chosen because they were shown¹⁸ to reproduce, to within 1 kcal/mol, the net activation barriers of gas-phase $\text{S}_{\text{N}}2$ identify exchange reactions involving methyl and benzyl halides that were calculated⁴² using the extremely rigorous focal-point approach. Moreover, density function theory calculations are not excessively computationally expensive, making it possible to carry out calculations on the large vinylogues.

Geometries were optimized for each reactant and transition state species involved in the parent (i.e., $n = 0$) methylation reactions and also the methylation reactions involving the $n = 1-5$ parallel vinylogues. For reactions involving the perpendicular vinylogues, geometries of the vinylogues were obtained by beginning with the optimized parallel vinylogue and rotating the terminal $\text{CH}=\text{CH}_2$ or $\text{CH}=\text{O}$ group 90° to the rest of the conjugated chain. For reactions involving the reference vinylogues, geometries of the vinylogues were obtained by beginning with the optimized parallel vinylogue and replacing the terminal $\text{CH}=\text{CH}_2$ or $\text{CH}=\text{O}$ group with a hydrogen atom.

Frequency calculations were carried out on all structures to provide each species' zero-point energy (ZPE). The ZPE-

corrected energies were used to calculate values of E^{b} for the various reactions. These frequency calculations also allowed us to ensure that there were no imaginary frequencies in the optimized reactants of the parent reactions, confirming that they were true energy minima, and that there was one imaginary frequency in each optimized transition state of the parent reactions, confirming that they were first-order saddle points.

Block-Localized Wave Function (BLW). The acetaldehyde enolate anion is described with two resonance structures, as shown previously in Scheme 1. In the resonance structures, a pair of π electrons is strictly localized on either the $\text{CH}=\text{CH}_2$ or $\text{CH}=\text{O}$ group and a lone pair is on the oxygen or carbon atom, leading to either O-methylation or C-methylation. In other words, our focus is on the π delocalization of the four π electrons. Thus, we can construct two BLWs corresponding to the two resonance structures by partitioning all orbitals and electrons into three blocks in each BLW computation. Two blocks are used for the four π electrons, while the third block involves all the remaining electrons and orbitals. The BLW method has been implemented in our in-house version of the quantum mechanical software GAMESS,⁴³ and all BLW computations were performed with the above optimal geometries at the B3LYP/6-311+G(d,p) level of theory. The comparison of the molecular energies computed with the standard B3LYP and the BLW methods manifests the impact of the resonance on the $\text{S}_{\text{N}}2$ reactions.

RESULTS AND DISCUSSION

Optimized Geometries. The optimized geometries for acetaldehyde enolate and the transition states for both O- and C-methylation are shown in Figure 5a-c. The geometries of the nucleophile and transition state of the reference reactions are shown in Figure 5d-g. In the transition state of O-methylation, we observe an anti conformation of the $\text{CH}=\text{CH}_2$ group and the reaction center about the enolate's C-O bond. In the transition state of C-methylation, the plane of the enolate anion is essentially perpendicular to the axis in which the new σ bond is

Table 1. Vinylogue Extrapolation Results for the O-Methylation [MPW1PW91/6-311++G(3df,3pd)]

n	$E_{\text{par}}^{\text{b}}$ (kcal/mol) ^a	$E_{\text{perp}}^{\text{b}}$ (kcal/mol) ^a	$E_{\text{ref}}^{\text{b}}$ (kcal/mol) ^a	$\Delta E_{\text{res}}^{\text{b}}$ (kcal/mol) ^a	$\Delta E_{\text{ind}}^{\text{b}}$ (kcal/mol) ^a	Hückel charge
0	11.9	N/A	-3.8	(-9.5) ^b	(-1.7) ^b	-0.76
1	18.5	12.4	11.9	-6.1 ^c	-0.5 ^d	-0.70
2	22.9	18.6	18.6	-4.3 ^c	0.0 ^d	-0.67
3	26.1	22.8	23.1	-3.3 ^c	0.3 ^d	-0.65
4	28.5	25.9	26.3	-2.7 ^c	0.4 ^d	-0.64
5	30.5	28.3	28.7	-2.2 ^c	0.5 ^d	-0.63

^a E^{b} refers to the net activation barrier depicted in Figure 2, which are potential energies including vibrational zero-point energies. ^bExtrapolated from the values calculated for $n = 1-5$ vinylogues. ^cContribution by resonance of the terminal CH=CH₂ group toward E^{b} of the n th vinylogue, computed as $E_{\text{perp}}^{\text{b}} - E_{\text{par}}^{\text{b}}$. ^dContribution by inductive effects of the terminal CH=CH₂ group toward E^{b} of the n th vinylogue, computed as $E_{\text{ref}}^{\text{b}} - E_{\text{perp}}^{\text{b}}$.

Table 2. Vinylogue Extrapolation Results for the C-Methylation [MPW1PW91/6-311++G(3df,3pd)]

n	$E_{\text{par}}^{\text{b}}$ (kcal/mol) ^a	$E_{\text{perp}}^{\text{b}}$ (kcal/mol) ^a	$E_{\text{ref}}^{\text{b}}$ (kcal/mol) ^a	$\Delta E_{\text{res}}^{\text{b}}$ (kcal/mol) ^a	$\Delta E_{\text{ind}}^{\text{b}}$ (kcal/mol) ^a	Hückel charge
0	13.0	N/A	-3.8	(-21.2) ^b	(-4.2) ^b	-0.33
1	20.8	7.8	4.4	-13.0 ^c	-3.4 ^d	-0.20
2	26.2	16.7	13.8	-9.5 ^c	-2.9 ^d	-0.15
3	30.0	22.4	20.0	-7.5 ^c	-2.4 ^d	-0.12
4	32.8	26.5	24.5	-6.3 ^c	-2.0 ^d	-0.10
5	35.0	29.6	27.8	-5.4 ^c	-1.8 ^d	-0.08

^a E^{b} refers to the net activation barrier depicted in Figure 2, which are potential energies including vibrational zero-point energies. ^bExtrapolated from the values calculated for $n = 1-5$ vinylogues. ^cContribution by resonance of the terminal CH=O group toward E^{b} of the n th vinylogue, computed as $E_{\text{perp}}^{\text{b}} - E_{\text{par}}^{\text{b}}$. ^dContribution by inductive effects of the terminal CH=O group toward E^{b} of the n th vinylogue, computed as $E_{\text{ref}}^{\text{b}} - E_{\text{perp}}^{\text{b}}$.

formed. Both of these optimized geometries are consistent with the ones reported by Lee and co-workers.⁴⁴

VE Results. Table 1 contains the MPW1PW91 calculated values of E^{b} for the S_N2 reactions involving the parallel, perpendicular, and reference vinylogues for O-methylation. Table 2 contains these values for C-methylation. In both tables, contributions by resonance [$\Delta E_{\text{res}}^{\text{b}}(n)$] and inductive effects [$\Delta E_{\text{ind}}^{\text{b}}(n)$] toward E^{b} are provided, which are computed using eqs 1 and 2, respectively. For each value of n , the Hückel charge at the nucleophilic atom of the reactant vinylogue is also listed. These Hückel charges were used for extrapolation of the $n = 1-5$ values of $\Delta E_{\text{res}}^{\text{b}}(n)$, as outlined later in the Discussion section. The values in parentheses are the $n = 0$ contributions by resonance or inductive effects, derived by extrapolation of the $n = 1-5$ values.

For both O- and C-methylation, the values of $\Delta E_{\text{res}}^{\text{b}}(n)$ computed for the $n = 1-5$ vinylogues become more negative with a decreasing value of n , indicating that the inclusion of resonance by the terminal CH=CH₂ and CH=O groups serves to increase the size of the energy barrier as n decreases. To extrapolate the $n = 1-5$ values back to $n = 0$ (the parent reactions), plots of $\Delta E_{\text{res}}^{\text{b}}(n)$ versus the Hückel calculated charge were constructed for both O-methylation and C-methylation (Figure 6). Both plots are quite linear, with R^2 values of 0.9958 and 0.9989, respectively. The resonance contribution for each parent reaction was computed by substituting the Hückel charge for $n = 0$ (Tables 1 and 2) into the appropriate linear equation: -0.76 for O-methylation and -0.33 for C-methylation. This yields a resonance contribution of -9.5 kcal/mol for O-methylation and -21.2 kcal/mol for C-methylation, as shown in parentheses in Tables 1 and 2.

The reasons for using the Hückel calculated charge for the fitting parameter of $\Delta E_{\text{res}}^{\text{b}}(n)$ were explained for our previous study on the benzylic effect.¹⁸ Briefly, it embodies the electrostatics at the reaction center, which, as Allen and co-workers⁴² pointed out, is the principal factor that scales with values of E^{b} for gas-phase S_N2 reactions. Moreover, Hückel

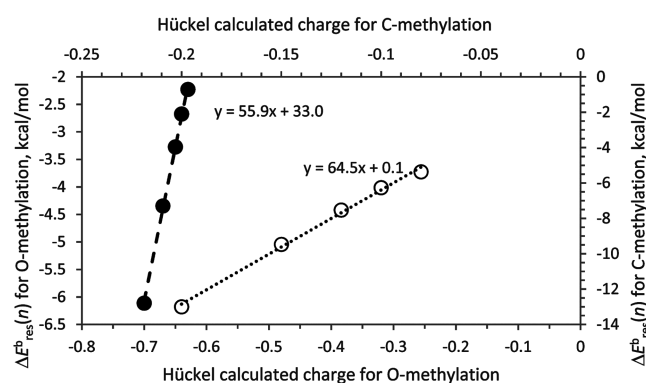


Figure 6. Plots of $\Delta E_{\text{res}}^{\text{b}}(n)$ versus the Hückel calculated charge. Calculated resonance contribution toward the net activation barrier for each vinylogue, $\Delta E_{\text{res}}^{\text{b}}(n)$, is plotted against the calculated Hückel charge at the nucleophilic atom. The results for the vinylogues of O-alkylation are shown using filled circles (●) and the corresponding x -axis is on the bottom, while the corresponding y -axis is on the left. The results for the vinylogues of C-alkylation are shown using unfilled circles (○) and the corresponding x -axis is on the top, while the corresponding y -axis is on the right.

theory, by design, takes into account effects only from π delocalization, which is what governs $\Delta E_{\text{res}}^{\text{b}}(n)$.

Like $\Delta E_{\text{res}}^{\text{b}}(n)$, values of $\Delta E_{\text{ind}}^{\text{b}}(n)$ become more negative for the $n = 1-5$ vinylogues as n decreases (Tables 1 and 2), reflecting an increasing contribution toward raising the net activation barrier with decreasing n . To extrapolate $\Delta E_{\text{ind}}^{\text{b}}(n)$ to $n = 0$ (i.e., the parent reactions), we take advantage of the expectation that inductive effects fall off exponentially with the distance between the substituent and the reaction center.^{16,21,45-50} Thus, the values of $\Delta E_{\text{ind}}^{\text{b}}(n)$ were plotted against n for both O-alkylation and C-alkylation, as shown in Figure 7, and were fit to the function: $\Delta E_{\text{ind}}^{\text{b}}(n) = A e^{-kn} + C$, where A , k , and C are fitting parameters. For O-methylation, these optimized parameters are $A = -2.18$, $k = -0.74$, and $C = 0.53$; for C-methylation, they are $A = -3.8$, $k = -0.21$, and $C = -0.40$. The curves in Figure 7 are the

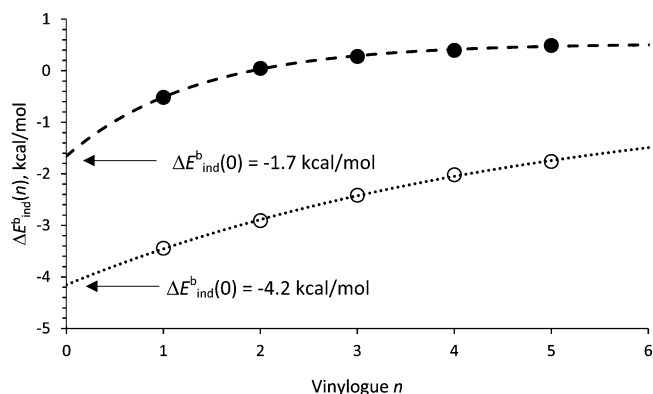


Figure 7. Plots of $\Delta E_{\text{ind}}^{\text{b}}(n)$ versus n . Calculated contribution by inductive effects toward the net activation barrier for each vinylogue, $\Delta E_{\text{ind}}^{\text{b}}(n)$, is plotted against n . The results for the vinylogues of O-alkylation are shown using filled circles (\bullet). The dashed line is the exponential function used to extrapolate these data, which was obtained from a nonlinear least-squares fit. The results for the vinylogues of C-alkylation are shown using unfilled circles (\circ). The dotted line is the exponential function used to extrapolate these data, which was obtained from a nonlinear least-squares fit.

optimized functions and reproduce the data very well. Substituting $n = 0$ into each linear equation yields the contribution by inductive effects toward E^{b} for the parent reactions, which are -1.7 kcal/mol for O-methylation and -4.2 kcal/mol for C-methylation.

BLW Results. We first examine the resonance in the free acetaldehyde enolate. At the optimized geometry of acetaldehyde enolate, the energies of two resonance structures compared with the real ground state, which is a hybrid of both resonance structures, are shown at the left of Figure 8. As the negative charge is substantially delocalized over the whole molecule in the hybrid, there is considerable π resonance in this anion. We calculate, in particular, that the hybrid is 49.9 kcal/mol lower in energy than the resonance structure with the negative charge localized on the oxygen atom (**R1**), and is 57.7 kcal/mol lower in

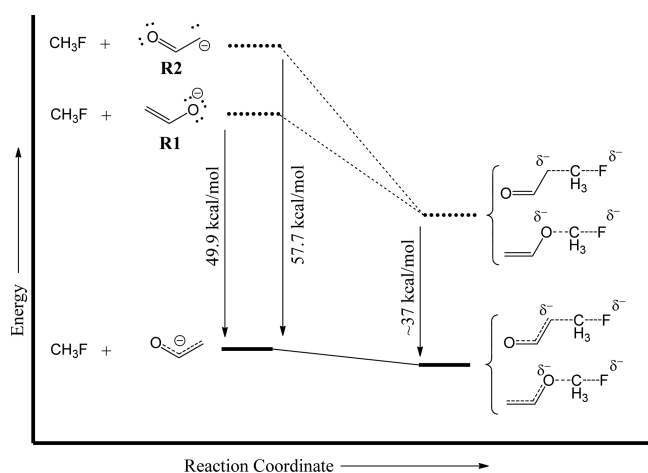


Figure 8. Contributions toward E^{b} with and without resonance in the enolate. Solid horizontal lines represent the energies of the electron-delocalized structures, and the dotted horizontal lines represent the electron-localized structures. Reactants are on the left, and transition structures are on the right. Each pair of delocalized and localized transition structures is calculated to be less than 2 kcal/mol different, so they are shown at the same energy to simplify the diagram.

energy than the resonance structure with the negative charge localized on the terminal carbon atom (**R2**). In other words, the former is more stable than the latter by 7.8 kcal/mol as a result of the higher electronegativity of oxygen than that of carbon, meaning that the latter has greater resonance energy.

We continue by examining the resonance contribution in the transition states for both O-methylation and C-methylation. Figure 9 shows resonance at the transition states using electron density difference (EDD) maps, which show the difference between the electron-localized state (BLW) and the electron-delocalized state (DFT). As expected, when resonance is turned on, the electron density moves from the negative charge center to either the $\text{CH}=\text{CH}_2$ or $\text{CH}=\text{O}$ group.

Table 3 compiles the energetic results of BLW computations of the transition states, which exhibit two notable findings. One is that resonance stabilizes the O- and C-methylation transition states by 37.1 and 35.4 kcal/mol, which are very close but significantly lower than their respective resonance energies in the free reactant acetaldehyde enolate anion (Figure 8). The other is, differently from the free enolate anion, at the transition states, **R1** has a little higher resonance energy than **R2**. Putting all the results together, we see that resonance increases the reaction barriers by 12.8 and 22.3 kcal/mol for the O- and C-methylation processes, as determined by $(49.9-37.1)$ and $(57.7-35.4)$, respectively.

Contributions by Resonance and Inductive Effects toward the Net Activation Barrier. The contributions by resonance toward the net activation barrier for the gas-phase $\text{S}_{\text{N}}2$ reaction of acetaldehyde enolate with methyl fluoride are substantially negative for both O- and C-methylation. For O-methylation, our VE results show that the contribution is -9.5 kcal/mol and our BLW results show that it is -12.8 kcal/mol. For C-methylation, those numbers from our VE and BLW results are -21.2 and -22.3 kcal/mol, respectively. The fact that these numbers are in such good agreement, despite coming from two completely different computational methodologies, provides substantial validation for our results.

The fact that these values are negative means that the net activation barrier is greater for the reactions involving the resonance-delocalized nucleophile and transition state than it is for the reactions in which resonance is effectively turned off. Such an outcome is rationalized by the notion that the formation of the new σ bond in the transition state is accompanied by a significant localization of the π electrons from the enolate anion into the reaction center. Therefore, the unrestricted delocalization that the free enolate anion enjoys is diminished in the transition state, so when resonance is effectively turned off, the enolate nucleophile suffers a rise in energy more than does the transition state. This is depicted in Figure 8.

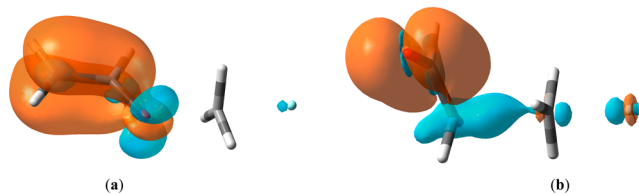


Figure 9. Electron density difference (EDD) maps showing the π conjugation at the transition states of (a) O-methylation (b) C-methylation. The orange color means an increase (gain) of electron density, while the cyan color shows a reduction (loss) of electron density (isodensity value 0.005 au).

Table 3. Energies of the Transition States in the S_N2 Reactions between Acetaldehyde Enolate Anion and CH_3F and the Contribution from the Resonance at the B3LYP/6-311+G Level**

mode	$E(\psi^{\text{DFT}})$ (au)	$E(\psi^{\text{BLW}})$ (au)	ΔE_{res} (kcal/mol)
O-attack	-292.91658	-292.85744	-37.1
C-attack	-292.91446	-292.85799	-35.4

The contributions by resonance toward E^b for O- and C-methylation are dominated by the contributions from resonance in just the free nucleophile. This is evidenced by our BLW calculations, which show that, upon going from the delocalized enolate nucleophile to each resonance structure in which the negative charge is localized on oxygen or carbon, energy rises by 49.9 or 57.7 kcal/mol, respectively. When we do the same for the transition state, those numbers are significantly smaller, at 37.1 and 35.4 kcal/mol, respectively. Similarly, in our $n = 1-5$ vinylogues, upon going from the parallel to the perpendicular conformation, the rise in energy is significantly greater for the free nucleophile than for the transition state, for both O-methylation and C-methylation. For the $n = 1$ vinylogues, for example, that rise in energy is 19.9 and 36.3 kcal/mol for the free enolates in O- and C-methylation, respectively. For the analogous transition states, those numbers are smaller, at 13.7 and 23.3 kcal/mol, respectively.

The greater resonance energies in the reactants than the transition states also explains why the resonance contribution toward E^b is greater for C-methylation than for O-methylation. The completely delocalized enolate anion has a greater π -electron density, and thus a greater concentration of negative charge, on the oxygen atom compared to the α carbon atom, owing to the greater electronegativity of oxygen. Therefore, the resonance structure with the negative charge on carbon represents a greater loss of delocalization and concomitant rise in energy than does the resonance structure with the negative charge on oxygen.

The effect that resonance has on E^b is analogous to what is seen in the gas-phase protonation of an enolate anion at either the oxygen or α carbon atom. Even though protonation at carbon leads to the thermodynamically favored product, protonation at oxygen is faster.^{51,52} As Bernasconi and Wenzel point out,⁵³ protonation at the α carbon atom requires significant charge localization in the transition state, which is partly responsible for the higher energy barrier. This loss of delocalization does not occur in the transition state when protonation takes place at oxygen.

In a qualitative sense, the fact that resonance favors O-methylation over C-methylation (by having a greater contribution toward E^b for C-methylation) is consistent with the principle of least nuclear motion. As Ofial and co-workers⁵⁴ point out, the resonance hybrid of the enolate anion resembles an enol ether (the product of O-methylation) more than it does an aldehyde (the product of C-methylation). Thus, O-methylation involves the "least change in atomic position and least change in electronic configuration."⁵⁵

Our resonance results are also in agreement with the qualitative argument put forth by Lee and co-workers,⁴⁴ in which they applied the principle of nonperfect synchronization. In their computational study of the gas-phase S_N2 reaction between acetaldehyde enolate and methyl fluoride, they identify a transition state imbalance in C-methylation, in which resonance develops early along the reaction coordinate and contributes to

an increase in the energy barrier. No such transition state imbalance is observed for O-methylation.

The contributions by inductive effects toward E^b are negative for both O- and C-methylation, indicating that inductive effects serve to increase the size of the energy barrier. This is consistent with the idea that electrostatics is the principal factor that scales with E^b , as outlined by Allen and co-workers.⁴² In the resonance structures of the enolate anion, the $\text{CH}=\text{CH}_2$ and $\text{CH}=\text{O}$ groups attached to the nucleophilic atom are both inductively electron withdrawing. Thus, these substituents serve to inductively remove negative charge from the respective oxygen and α carbon atoms. This leads to a diminished electrostatic stabilization between the nucleophilic atom and the electrophilic carbon of CH_3F in the transition state. Consequently, the size of the energy barrier increases.

The contribution by inductive effects is greater in C-methylation than in O-methylation: -4.2 kcal/mol for the former and -1.7 kcal/mol for the latter. This is consistent with the $\text{CH}=\text{O}$ substituent being a stronger electron withdrawing group inductively than $\text{CH}=\text{CH}_2$. Indeed, the Swain-Lupton field parameter⁵⁶ of $\text{C}(\text{CH}_3)=\text{O}$ is 0.33 and that of $\text{CH}=\text{CH}_2$ is 0.13, reflective of the greater electronegativity of oxygen than that of carbon.

We note that the contributions by resonance (-9.5 to -12.8 kcal/mol) and inductive effects (-1.7 kcal/mol) toward E^b for O-methylation sum to -11.1 to -14.3 kcal/mol. We also note that the calculated difference in E^b for O-methylation of acetaldehyde enolate and the reaction between HO^- and CH_3F is -15.7 kcal/mol (Table 1). Thus, the contributions by resonance and inductive effects that we calculate for O-methylation can account for essentially the entirety of that increase in the size of the energy barrier.

The story is somewhat different for C-methylation. Our results show that the contributions by resonance (-21.2 to -22.3 kcal/mol) and inductive effects (-4.2 kcal/mol) sum to -25.4 to -26.4 kcal/mol. The calculated difference in E^b between C-methylation of acetaldehyde enolate and the reaction of H_3C^- with CH_3F is -16.8 kcal/mol. Thus, there appears to be another significant contribution in C-methylation of acetaldehyde enolate that serves to counteract the increase in E^b stemming from resonance and inductive effects. We believe that this is due, at least in part, to the fact that the geometry of the α carbon in the enolate anion is different from the geometry of the carbon atom in H_3C^- as shown in Figure 5. In H_3C^- , the carbon atom is sp^3 -hybridized and pyramidal, whereas the α carbon in acetaldehyde enolate is sp^2 -hybridized and planar. Our H_3C^- reference vinylogues were constructed by replacing the terminal $\text{CH}=\text{O}$ group of an acetaldehyde enolate vinylogue with a hydrogen atom, thereby preserving the planar geometry at the α carbon. This was done deliberately so that our values of ΔE_{ind}^b calculated for each vinylogue reflect only the inductive contributions by the terminal $\text{CH}=\text{O}$ group, not changes in geometry at the nucleophilic carbon. Thus, the contribution by inductive effects that we obtained by extrapolating the ΔE_{ind}^b values of the vinylogues should embody that enforced planarity, giving rise to the discrepancy described above.

CONCLUSIONS

Employing our VE and BLW methodologies, we determined that, for the gas-phase S_N2 reaction between acetaldehyde enolate and methyl fluoride, resonance is the dominant factor that leads to O-methylation being favored over C-methylation, and inductive effects are significant. Resonance serves to increase

the net activation barrier for O-methylation by roughly 9.5–12.8 kcal/mol, whereas it serves to increase the net activation barrier for C-methylation by roughly 21.2–22.3 kcal/mol. Inductive effects also contribute significantly toward increasing the size of the net activation barrier for each reaction: roughly 1.7 kcal/mol for O-methylation and 4.2 kcal/mol for C-methylation. For O-methylation, these resonance and inductive effects account for essentially the entire difference between the net activation barrier involving acetaldehyde enolate as the nucleophile relative to hydroxide anion as the nucleophile. For C-methylation, the difference in net activation barriers between the reaction involving acetaldehyde enolate and methanide anion is smaller than the sum of our calculated resonance and inductive effects. This suggests that, for C-methylation, there is another factor that contributes toward lowering the net activation barrier, which we attribute to the different hybridizations of the α carbon of acetaldehyde enolate and of the carbon atom in methanide anion.

■ ASSOCIATED CONTENT

📄 Supporting Information

The Supporting Information is available free of charge on the ACS Publications website at DOI: [10.1021/acs.joc.6b00351](https://doi.org/10.1021/acs.joc.6b00351).

Cartesian coordinates, absolute energies, zero-point energies, and number of imaginary frequencies for each calculated structure (PDF)

■ AUTHOR INFORMATION

Corresponding Authors

*E-mail: yirong.mo@wmich.edu

*E-mail: jkarty@elon.edu

Notes

The authors declare no competing financial interest.

■ ACKNOWLEDGMENTS

J.M.K. would like to thank the U.S. National Science Foundation for support of this research, under the Grant No. CHE-1058833. Y.M. acknowledges the support from the U.S. National Science Foundation under the Grant No. CNS-1126438. H.Z. acknowledges the financial support from the China Scholarship Council (CSC). Financial support for C.G.S. was provided by the Elon University Lumen Prize, the Elon University Undergraduate Research Program, and the Glen Raven scholarship.

■ REFERENCES

- (1) Smith, M. B.; March, J. In *Advanced Organic Chemistry: Reactions, Mechanisms and Structure*; 5th ed.; John Wiley & Sons, Inc.: New York, 2001; p 551.
- (2) Contreras, R.; Domingo, L. R.; Andrés, J.; Pérez, P.; Tapia, O. *J. Phys. Chem. A* **1999**, *103*, 1367.
- (3) Jones, M. E.; Kass, S. R.; Filley, J.; Barkley, R. M.; Ellison, G. B. *J. Am. Chem. Soc.* **1985**, *107*, 109.
- (4) Sakata, T.; Seki, N.; Yomogida, K.; Yamagishi, H.; Otsuki, A.; Inoh, C.; Yamataka, H. *J. Org. Chem.* **2012**, *77*, 10738.
- (5) Houk, K. N.; Paddon-Row, M. N. *J. Am. Chem. Soc.* **1986**, *108*, 2659.
- (6) Brauman, J. I.; Blair, L. K. *J. Am. Chem. Soc.* **1970**, *92*, 5986.
- (7) Zhong, M.; Brauman, J. I. *J. Am. Chem. Soc.* **1996**, *118*, 636.
- (8) Albery, W. J. *Annu. Rev. Phys. Chem.* **1980**, *31*, 227.
- (9) Marcus, R. A. *Annu. Rev. Phys. Chem.* **1964**, *15*, 155.
- (10) Marcus, R. A. *J. Phys. Chem.* **1968**, *72*, 891.
- (11) Marcus, R. A. *J. Am. Chem. Soc.* **1969**, *91*, 7224.
- (12) Marcus, R. A. *Angew. Chem.* **1993**, *105*, 1161.
- (13) Marcus, R. A. *Pure Appl. Chem.* **1997**, *69*, 13.
- (14) Breugst, M.; Zipse, H.; Guthrie, J. P.; Mayr, H. *Angew. Chem., Int. Ed.* **2010**, *49*, 5165.
- (15) Hoz, S.; Bosch, H.; Wolk, J. L.; Hoz, T.; Rosental, E. *J. Am. Chem. Soc.* **1999**, *121*, 7724.
- (16) Barbour, J. B.; Karty, J. M. *J. Org. Chem.* **2004**, *69*, 648.
- (17) Olmstead, W. N.; Brauman, J. I. *J. Am. Chem. Soc.* **1977**, *99*, 4219.
- (18) Rawlings, R. E.; McKerlie, A. K.; Bates, D. J.; Mo, Y.; Karty, J. M. *Eur. J. Org. Chem.* **2012**, *2012*, 5991.
- (19) Dworkin, A.; Naumann, R.; Seigfred, C. *J. Org. Chem.* **2005**, *70*, 7605.
- (20) Fersner, A.; Karty, J. M.; Mo, Y. *J. Org. Chem.* **2010**, *75*, 522.
- (21) Holt, J.; Karty, J. M. *J. Am. Chem. Soc.* **2003**, *125*, 2797.
- (22) Pauling, L. C. *The Nature of the Chemical Bond*; 3rd ed.; Cornell University Press: Ithaca, NY, 1960.
- (23) Wheland, G. W. *Resonance in Organic Chemistry*; Wiley: New York, 1955.
- (24) *Valence Bond Theory*; Cooper, D. L., Ed.; Elsevier: Amsterdam, 2002.
- (25) Gallup, G. A. *Valence Bond Methods: Theory and Applications*; Cambridge University Press: New York, 2002.
- (26) Shaik, S. S.; Hiberty, P. C. *A Chemist's Guide to Valence Bond Theory*; Wiley-Interscience: New York, 2007.
- (27) Wu, W.; Su, P.; Shaik, S.; Hiberty, P. C. *Chem. Rev.* **2011**, *111*, 7557.
- (28) Stoll, H.; Preuss, H. *Theor. Chim. Acta* **1977**, *46*, 11.
- (29) Stoll, H.; Wagenblast, G.; Preuss, H. *Theor. Chim. Acta* **1980**, *57*, 169.
- (30) Mehler, E. L. *J. Chem. Phys.* **1977**, *67*, 2728.
- (31) Mehler, E. L. *J. Chem. Phys.* **1981**, *74*, 6298.
- (32) Gianinetti, E.; Raimondi, M.; Tornaghi, E. *Int. J. Quantum Chem.* **1996**, *60*, 157.
- (33) Gianinetti, E.; Vandoni, I.; Famulari, A.; Raimondi, M. *Adv. Quantum Chem.* **1998**, *31*, 251.
- (34) Famulari, A.; Gianinetti, E.; Raimondi, M.; Sironi, M. *Int. J. Quantum Chem.* **1998**, *69*, 151.
- (35) Khaliullin, R. Z.; Cobar, E. A.; Lochan, R. C.; Bell, A. T.; Head-Gordon, M. *J. Phys. Chem. A* **2007**, *111*, 8753.
- (36) Mo, Y.; Peyerimhoff, S. D. *J. Chem. Phys.* **1998**, *109*, 1687.
- (37) Mo, Y.; Song, L.; Lin, Y. *J. Phys. Chem. A* **2007**, *111*, 8291.
- (38) Mo, Y. In *The Chemical Bond: Fundamental Aspects of Chemical Bonding*; Frenking, G., Shaik, S., Eds.; Wiley-VCH: Weinheim, Germany, 2014.
- (39) Frisch, M. J.; Trucks, G. W.; Schlegel, H. B.; Scuseria, G. E.; Robb, M. A.; Cheeseman, J. R.; Scalmani, G.; Barone, V.; Mennucci, B.; Petersson, G. A.; Nakatsuji, H.; Caricato, M.; Li, X.; Hratchian, H. P.; Izmaylov, A. F.; Bloino, J.; Zheng, G.; Sonnenberg, J. L.; Hada, M.; Ehara, M.; Toyota, K.; Fukuda, R.; Hasegawa, J.; Ishida, M.; Nakajima, T.; Honda, Y.; Kitao, O.; Nakai, H.; Vreven, T.; Montgomery, Jr., J. A.; Peralta, J. E.; Ogliaro, F.; Bearpark, M. J.; Heyd, J.; Brothers, E. N.; Kudin, K. N.; Staroverov, V. N.; Kobayashi, R.; Normand, J.; Raghavachari, K.; Rendell, A. P.; Burant, J. C.; Iyengar, S. S.; Tomasi, J.; Cossi, M.; Rega, N.; Millam, N. J.; Klene, M.; Knox, J. E.; Cross, J. B.; Bakken, V.; Adamo, C.; Jaramillo, J.; Gomperts, R.; Stratmann, R. E.; Yazyev, O.; Austin, A. J.; Cammi, R.; Pomelli, C.; Ochterski, J. W.; Martin, R. L.; Morokuma, K.; Zakrzewski, V. G.; Voth, G. A.; Salvador, P.; Dannenberg, J. J.; Dapprich, S.; Daniels, A. D.; Farkas, Ö.; Foresman, J. B.; Ortiz, J. V.; Cioslowski, J.; Fox, D. J.; *Gaussian 09*; Gaussian, Inc.: Wallingford, CT, 2009.
- (40) Dennington, R.; Keith, T.; Millam, J.; *GaussView5*; Semichem Inc.: Shawnee Mission, KS, 2009.
- (41) Adamo, C.; Barone, V. *J. Chem. Phys.* **1998**, *108*, 664.
- (42) Galabov, B.; Nikolova, V.; Wilke, J. J.; Schaefer, H. F., III; Allen, W. J. *J. Am. Chem. Soc.* **2008**, *130*, 9887.
- (43) Schmidt, M. W.; Baldrige, K. K.; Boatz, J. A.; Elbert, S. T.; Gordon, M. S.; Jensen, J. J.; Koseki, S.; Matsunaga, N.; Nguyen, K. A.; Su, S.; Windus, T. L.; Dupuis, M.; Montgomery, J. A. *J. Comput. Chem.* **1993**, *14*, 1347.
- (44) Lee, B.-S.; Kim, C. K.; Kim, C. K.; Han, I.-S.; Park, H. Y.; Lee, I. *Bull. Korean Chem. Soc.* **1999**, *20*, 559.

- (45) Barbour, J. B.; Karty, J. M. *J. Phys. Org. Chem.* **2005**, *18*, 210.
- (46) Bianchi, G.; Howarth, O. W.; Samuel, C. J.; Vlahov, G. *J. Chem. Soc., Perkin Trans. 2* **1995**, *7*, 1427.
- (47) Branch, G. E.; Calvin, M. *The Theory of Organic Chemistry*; Prentice Hall: New York, 1941.
- (48) McGowan, J. C. *Nature* **1947**, *159*, 644.
- (49) Peterson, P. E.; Casey, C. *Tetrahedron Lett.* **1963**, *4*, 1569.
- (50) Stock, L. M. *J. Chem. Educ.* **1972**, *49*, 400.
- (51) Zimmerman, H. E. *Acc. Chem. Res.* **1987**, *20*, 263.
- (52) Brauman, J. I.; Lieder, C. A.; White, M. J. *J. Am. Chem. Soc.* **1973**, *95*, 927.
- (53) Bernasconi, C. F.; Wenzel, P. J. *J. Am. Chem. Soc.* **1994**, *116*, 5405.
- (54) Mayr, H.; Breugst, M.; Ofial, A. R. *Angew. Chem., Int. Ed.* **2011**, *50*, 6470.
- (55) Rice, F. O.; Teller, E. *J. Chem. Phys.* **1938**, *6*, 489.
- (56) Hansch, C.; Leo, A.; Taft, R. W. *Chem. Rev.* **1991**, *91*, 165.